Journal of Nuclear Materials 496 (2017) 362–366

Contents lists available at ScienceDirect

Journal of Nuclear Materials

journal homepage: www.elsevier.com/locate/jnucmat

Dislocation core structures of tungsten with dilute solute hydrogen

Yinan Wang [a], Qiulin Li [b], Chengliang Li [c], Guogang Shu [c], Ben Xu [a, *], Wei Liu [a, **]

[a] Key Laboratory of Advanced Materials (MOE), School of Material Science and Engineering, Tsinghua University, Beijing 100084, China
[b] Graduate School at Shenzhen, Tsinghua University, Shenzhen, China
[c] State Key Laboratory of Nuclear Power Safety Monitoring Technology and Equipment, China Nuclear Power Engineering Co., Ltd., Shenzhen 518172, China

ARTICLE INFO

Article history:
Received 28 February 2017
Received in revised form
11 September 2017
Accepted 13 September 2017
Available online 18 September 2017

Keywords:
Screw dislocation
Edge dislocation
QM/MD method
Stacking fault energy

ABSTRACT

In this paper, a combination of quantum mechanical and interatomic potential-based atomistic calculations are used to predict the core structures of screw and edge dislocations in tungsten in the presence of a particular concentration of hydrogen atoms. These configurations of the core structures are the results of two competing energies: the interaction between the partial dislocations and the corresponding generalized stacking fault energy in between the two partial dislocations, which are presented in this work. With this, we can precisely predict the configurations of the hydrogen-doped dislocation core structures.

1. Introduction

With recent developments in thermonuclear fusion research, tungsten has emerged as one of the most promising plasma-facing materials (PFM). As a PFM, tungsten may be subjected to high magnitudes of heat and particle flux of hydrogen isotopes escaping from the plasma, which would promote the growth of cracks and ultimately result in the deformation and failure of the tungsten. One of the origins of the degradation of mechanical properties is the microscopic changes in the dislocation behavior. In recent MD simulations, the edge dislocations in Ni have been used to demonstrate that hydrogen may influence the distance between partial dislocations [1]. Additionally, the hydride-to-non-hydride transformation could be correlated to the nucleation of microcracks at the tips of dislocation pile-ups [2]. According to the results of another MD simulation performed on Fe, a high concentration of hydrogen imparts a unique core structure to screw dislocations, while in edge dislocations, the core energy and Peierls potential decrease as a function of the hydrogen concentration [3]. In the DFT work of D. Terentyev et al. [4], the authors demonstrated that H atoms are strongly bound to the screw dislocation core in body-centered cubic (bcc) W and exhibit fast one-dimensional migration along the dislocation line. Additionally, they observed the formation of a jog on the dislocation line introduced by the transformation of a cluster of eight H atoms into an immobile configuration. Another MD work by Petr Grigorev et al. [5] suggested a strong and localized attraction of H to the core of edge dislocations, although the results fully depend on the potentials. To summarize the limitation of the above research, the empirical potentials for MD calculations [6] were not developed specifically to include the interactions between hydrogen and dislocation cores in tungsten, and thus, the possible deviated structure could be predicted. Moreover, it is still a challenge for DFT simulation due to the long range stress field of edge dislocations. Therefore, a reliable algorithm that suitably includes the interactions between dislocations and hydrogen atoms is needed for the prediction of core structures. With this, it is highly recommend to evaluate the dislocation core structures in the presence of H atoms as empirical potentials are developed in the future. Additionally, since the mobility of dislocations is strongly dependent on their core structure, such work substantially increases our ability to understand the possible mechanism of hydrogen embrittlement in tungsten.

2. Method

2.1. QM/MD method

In this paper, a systematic study using a quantum mechanics/

* Corresponding author.
** Corresponding author.
E-mail addresses: xuben@mail.tsinghua.edu.cn (B. Xu), liuw@tsinghua.edu.cn (W. Liu).

https://doi.org/10.1016/j.jnucmat.2017.09.019
0022-3115/

molecular mechanics (QM/MD) [7] method determines the stable core structures of screw and edge dislocations with a certain concentration of hydrogen atoms. Then, the generalized stacking fault energy (γ_{SFE}) is discussed to characterize the influence of hydrogen on γ_{SFE}, which is vital for understanding the non-split phenomenon in the cores of edge dislocations in the presence of hydrogen atoms. To obtain insight into the dislocation core structures, a QM/MD method is used, which divides the system into two regions: the core of the dislocation (I) and the surrounding area (II). In this way, the dislocation core is precisely described by an ab initio method, while the other parts of the dislocation are described using the molecular mechanics (MD) method. This circumvents the difficulties of choosing a proper potential to describe the dislocation core or of simultaneously dealing with different elements. Meanwhile, the size of the dislocation model is not limited by the QM method because the MD method is used for large-scale descriptions of atoms. Additionally, the accuracy of calculations is guaranteed by inserting a boundary part, B, which reduces the coupling of errors between the two regions. The simulation process is presented in Fig. 1. The initial dislocation structure predicted by the theoretical displacement field [8] was used as the input. The QM method is applied to the description of region I as the atoms in region B are fixed. In region II, the MD method is used to minimize the total energy and the atomic force as the atoms in region I and region B are immobilized. The MD method is also used to describe region B, but in this case, the atoms in region I and II are pinned. The total energy and the force on each atom are checked at each step of the relaxation. The energy convergence threshold for self-consistent-field iteration is set at 10-4 eV. The atomic positions are fully optimized until all the residual forces are smaller than 0.001 eV $Å^{-1}$.

2.2. Dislocation model

Regarding the models employed in the calculations, the screw and edge dislocations are placed at the cores of two separate cuboids. Considering an isolated 1/2 ⟨111⟩ screw dislocation, the X, Y, and Z axes are set as [112], [1$\bar{1}$0], and [11$\bar{1}$], respectively. The Burgers vector is along the Z axis, set as a/2[11$\bar{1}$]. Similarly, an

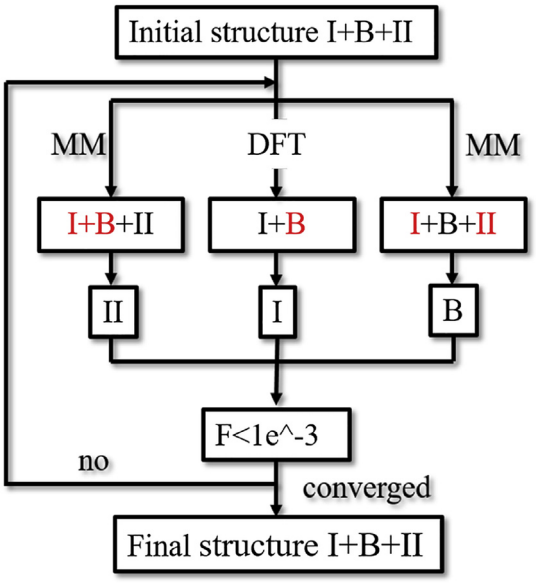

Fig. 1. The simulation procedure of the QM/MD method. Red color denotes the fixed region during a certain step of relaxation. (For interpretation of the references to colour in this figure legend, the reader is referred to the web version of this article.)

1/2⟨111⟩ {011} isolated edge dislocation is built, where the X, Y, and Z directions of the simulation cell correspond to the Burgers vector a/2[111], the normal direction of the slip plane [$\bar{1}$10], and the dislocation line [$\bar{1}\bar{1}$2], respectively. Due to the aperiodic nature of both dislocations, a periodic boundary condition is used along only the z direction, which is the direction of the dislocation line. The cell dimensions for the screw dislocation are 390.45, 387.73, and 11.04 Å along the X, Y, and Z directions, respectively; and those in the edge dislocation are 552.18, 559.06, and 15.62 Å along the X, Y and Z directions, respectively. The total numbers of atoms are 101572 in the screw dislocation and 296856 in the edge dislocation. For a screw/edge dislocation, 180/234 atoms are in the DFT region, with 92/128 inner atoms handled using the DFT method and 88/106 outer atoms fixed during the simulation. In addition, we enlarged the boundary part to 372/771 atoms, but the outer atoms were not included during the DFT simulation because of the limited atom numbers on which the DFT method could work. These numbers can reasonably yield converged results with respect to both the dislocation core structure and its stress field. To create the dislocations, the atoms are displaced by isotropic and linear elastic fields. A column of H atoms (denoting the periodic boundary condition along the z direction) is added to the tetrahedral interstitial site nearest to the screw dislocation core, which is the most stable position [4]. In the case of the edge dislocation, the H atoms are directly set at the space below the extra half-plane of atoms, which acts as a trap for interstitial atoms. The concentration of the H atoms in the screw and edge dislocations are 0.09/nm and 0.06/nm, respectively.

2.3. Details of simulation

The QM calculations were performed within the spin-polarized generalized gradient approximation (GGA) [9] via the Vienna Ab initio Simulation Package (VASP) [10–12]. Ultrasoft pseudopotentials were used in the simulations. Blochs projector augmented-wave (PAW) [13] method was employed to describe the interactions between ions and electrons. Brillouin zone sampling was carried out using the Monkhorst-Pack Scheme [14]. In both situations, the k-points are selected as 1 1 2, and the energy cut-off is set as 350 eV. A semi-empirical embedded atom method (EAM) based on a potential developed by X. W. Zhou et al. [15], a modified embedded atom method (MEAM) potential developed by D Cereceda et al. [16] and the WCH-tersoff potential developed by X Yang [6,17] were adopted for the MD simulations. The potentials were scaled such that the potentials yielded precisely the same lattice constant and bulk modulus as that of bcc W simulated by the QM method [18]. The MD simulation was carried out by integrating Newton's equations of motion through the LAMDPS code [19]. The time step was set at 1 fs. The H-dislocation binding energy was computed as [20,21] $E_b = (E_{H+dis} + E_{bulk}) - (E_{dis} + E_H)$, in which E_{H+dis}, E_{dis}, and E_H are the total energy of the crystals containing H and dislocation simultaneously, only the dislocation and only the H atom, respectively. E_{bulk} is the total energy of the perfect W crystal with the same dimensions as used to model the dislocation. A negative E_b implies that a system gains energy due to the association of objects. Therefore, an attractive interaction between two objects will correspond to a negative binding energy.

3. Results

3.1. Screw dislocation

Fig. 2(a–b) reveals the screw dislocation structures predicted by the MD method employing different potentials and the QM/MD method. Our differential displacement (DD) maps show the atomic

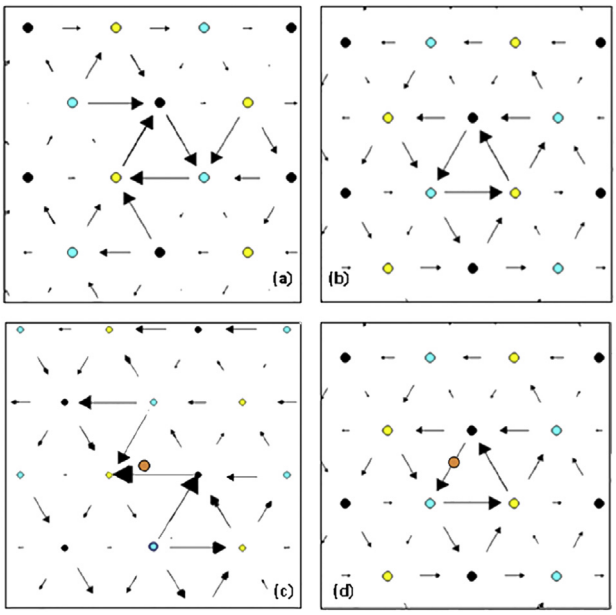

Fig. 2. Tungsten screw dislocation DD maps [17] predicted by the MD method and QM/MD method. (a) Result of the MD method employing the EAM potential; (b) result of the MD method employing the MEAM potential and the QM/MD method; (c) the core of the screw dislocation with a column of hydrogen atoms (orange circle) predicted by the MD method employing the WCH-tersoff potential and (d) the QM/MD method. The Burgers vector is a/2[111], and different colors represent the different layers of atoms. The length of the arrows is proportional to the magnitude of displacement. (For interpretation of the references to colour in this figure legend, the reader is referred to the web version of this article.)

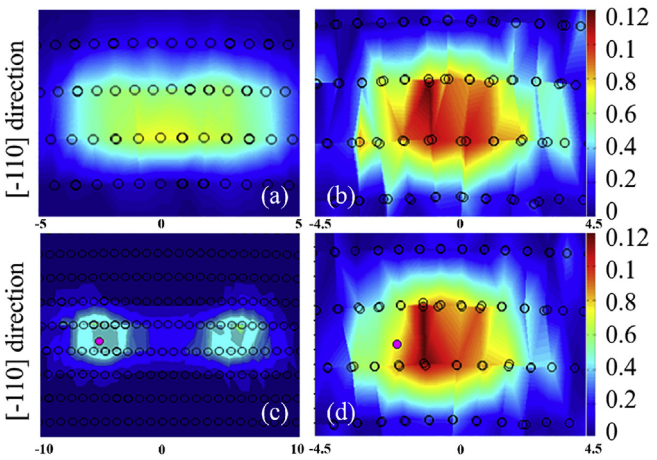

Fig. 3. The Nye tensor diagrams of edge dislocations predicted by (a) the MD method employing the EAM potential; (b) the MD method employing the MEAM potential and the QM/MD method; the edge dislocation core with a column of hydrogen atoms (pink circle) predicted by (c) the MD method employing the WCH-tersoff potential and (d) the QM/MD method. The Burgers vector is a/2[111], displayed in different colors, and the black circles denote the atoms. As the color changes from blue to red, the ratio between the norm of the local Burgers vector and an ideal Burgers vector becomes larger. (For interpretation of the references to colour in this figure legend, the reader is referred to the web version of this article.)

structure projected onto the (111) plane. Fig. 2(a) revealed that for the EAM potential, the screw dislocation core is spread asymmetrically, splitting into three adjacent {211} planes [22]. As revealed in Fig. 2(b), the MEAM potential and the QM/MD method provided the same results, as the screw dislocation is non-degenerate, expanding equally along the six ⟨112⟩ directions. This is called the easy-core configuration [23], which is a typical non-polarized core, implying the stability of the configuration. This easy core has an approximately threefold rotational point group symmetry about the [111] axis through the center of the map. After inserting a column of hydrogen atoms, the MD method predicted a quite different result from the QM/MD method. Fig. 2(c) presents a split core structure from the MD method employing the WCH-tersoff potential. In contrast, the QM/MD method suggests that the H atoms did not disturb the core structure significantly, as shown in Fig. 2(d), because the volume of the hydrogen atoms is not large enough to distort the tungsten lattice. The binding energy of H to the screw dislocation core is calculated as −0.55eV, which is in good agreement with the previous study [4].

3.2. Edge dislocation

The edge components of the Nye tensor [24,25] for the results obtained from the MD method and the QM/MD method are shown in Fig. 3(a–b). In Fig. 3(a), the Nye tensor has a wide distribution in the core predicted by the EAM potential. Instead, in Fig. 3(b), a narrower distribution was given by the MEAM potential and the QM/MD method, particularly in the tensile field of the dislocation. Fig. 3(c–d) displayed the structures with the addition of hydrogen atoms. In Fig. 3(c), the WCH-tersoff potential revealed a splitting behavior of the dislocation core, which remained in doubt because such phenomena were not investigated in previous simulations or experiments. Accordingly, in Fig. 3(d) the QM/MD method predicted a structure that is not significantly changed by the H atom because of the limited concentration. The binding energy predicted by the QM/MD method is found to be −0.9548 eV, which is comparable with the result from Grigorev's work [5]. The negative value of the binding energy indicated that the impurity atom H prefers to segregate to the dislocation core as opposed to staying in the bulk, while the edge dislocation is more attractive to H than the screw dislocation. Our results are significantly different from the dislocation core structures predicted by the WCH-tersoff potential, especially in the splitting behavior of the dislocation cores.

4. Discussion

To discuss the stacking fault energy, we simply carried out the QM simulation because the stress field is described by the periodic boundary conditions precisely and the system employed consists of few atoms. In addition, the MD method was considered here to assess whether the potential could successfully predict the properties of the stacking fault energy and the attributes of dislocations. The QM/MD method was not included here. The block shearing process was carried out with a supercell consisting of 12 atomic planes in the direction perpendicular to the cut. The crystal was oriented along the following axes: x = [111], y = [$\bar{1}$10], and z = [$\bar{1}$12]. The results of the surface convergence tests implied that a $2 \times 12 \times 2$ bulk could be the model for simulation (Fig. 4(a)). The crystal was divided into two parts along the [$\bar{1}$10] diagonal direction. To simulate the slip behavior of the edge dislocation on the {110} plane using a step of 0.05b, where b = a/2 [111] is the Burgers vector in a bcc crystal, the lower part was fixed, while the upper part was gradually displaced in the [111] direction in a stepwise manner. The simulation procedure is as follows [26]: $D_1 = U_1 - U_0$ is the relative shear displacement between the fixed lower part and the first neighboring plane, $D_2 = U_2 - U_1$ is the relative shear displacement between the second and the first atomic planes above the fixed part, and $D_3 = U_3 - U_2$ is defined similarly. The generalized stacking fault energy is therefore simulated as follows:

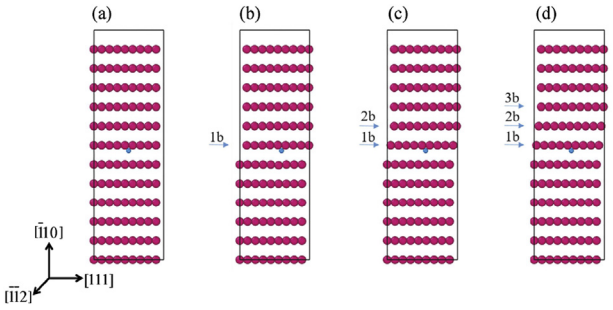

Fig. 4. Atomic configurations of the bulk W (a) employed in the stacking fault energy calculation. The pink atoms are tungsten atoms, and the small blue atom is the inserted hydrogen atom. The diagrams of the 1SF (b), 2SF (c), and 3SF (d) models reveal the procedure of producing different types of stacking faults, in which the upper parts of the atoms are moved along the [111] direction in distinct manners. (For interpretation of the references to colour in this figure legend, the reader is referred to the web version of this article.)

$$\gamma_{SFE}(u) = \frac{E(u) - E_0}{A} \tag{1}$$

where A is the square of the slip plane. Three different types of stacking faults are considered:

(1) 1SF: $D_1 \neq 0, D_2 = D_3 = 0$
(2) 2SF: $D_1 = D_2 \neq 0, D_3 = 0$
(3) 3SF: $D_1 = D_2 = D_3 \neq 0$

The formation of 1SF, 2SF, and 3SF is shown in Fig. 4(b–d). A column of hydrogen atoms is added to a tetrahedral interstice in the first neighboring plane above the fixed part and is tested by detailed calculations. We first checked how the divergent methods predicted the stacking fault energy differently, as shown in Fig. 5(a). During the simulation, the atoms were relaxed normal to the stacking fault energy plane. Clearly, the WCH-tersoff potential failed to predict the reliable stacking fault energy curves in both values and shape, which is consistent with the appearance of the dislocation structures in the previous results. The EAM potential predicted an unimodel curve, despite the sharp peak revealing that it overestimated the stacking fault energy as 2523.4 mJ/m^2. The result of the MEAM potential fits quite well with the DFT method, as both of them determined the stacking fault energy as approximately 1650 mJ/m^2, which is consistent with a former publication [27], further proving that the MEAM potential could predict the behavior of the dislocations properly. Changes in the generalized stacking fault energy (γ_{SFE}) during the rigid sliding of the upper (moving) and lower (fixed) part of the crystal along the [111] direction for various values of the displacements D_1/b, D_2/b, and D_3/b are shown in Fig. 5(b). In the generation of the stacking fault 1SF, the highest lattice resistance occurs at $D_1 = 0.5$, and the maximum of γ_{SFE} is 1649.3 mJ/m^2. Here, γ_{SFE} represents the unstable stacking fault energy, which is the energy barrier for generating a fully developed edge dislocation in this slip system. There are no other energy minima, indicating that no intrinsically stable SFs exist. The maximum of γ_{SFE} is 2969.91 mJ/m^2 in 2SF and 4224.45 mJ/m^2 in 3SF. Neither of them are stable in the slip system because there are no local metastable minima. The addition of a column of hydrogen atoms resulted in the decrease in γ_{SFE} for 1SF to 1483.34 mJ/m^2 and had similar influences on 2SF and 3SF. However, the H atoms neither decreased the γ_{SFE} to a certain value, which could lead to a stacking fault, nor introduced another local metastable minimum, indicating that a finite amount of hydrogen atoms have a limited influence on the γ_{SFE} of the tungsten and on the structure of the edge dislocation. Comparable conclusions were drawn from the simulations of the edge dislocations.

Since the spacing between partials is defined by the balance between repulsive forces acting between the partial dislocations and attractive force due to the stacking fault energy γ, we further employed the following method to calculate the forces between parallel dislocations in the same glide plane with $b_2(\frac{a}{4}[111])$ and $b_3(\frac{a}{4}[111])$ by considering the interactions between their edge components [28]:

$$\begin{aligned}\overrightarrow{F_e} &= \frac{G\left(\overrightarrow{b_2}\cdot\overrightarrow{b_3}\right)}{2\pi(1-\nu)}\cdot\frac{x(x^2-y^2)}{\left(x^2+y^2\right)^2} \\ &= \frac{G\left(\overrightarrow{b_2}\cdot\overrightarrow{b_3}\right)}{2\pi(1-\nu)d} = \frac{3G\cdot a^2}{32\pi(1-\nu)d}\end{aligned} \tag{2}$$

where d represents the distance between the partial dislocations; G denotes the bulk modulus, which is 160 Gpa here [29]; and ν is the Poisson ratio and has a value of 0.28 [30]. The stacking fault energy γ [mJ/m^2] acts against the expansion of the stacking fault region, with γ being the force acting on a unit length of a dislocation. If we could observe partial dislocations, the approximate equilibrium separation d could be found as:

$$d < \frac{3G\cdot a^2}{32\pi(1-\nu)\gamma} \tag{3}$$

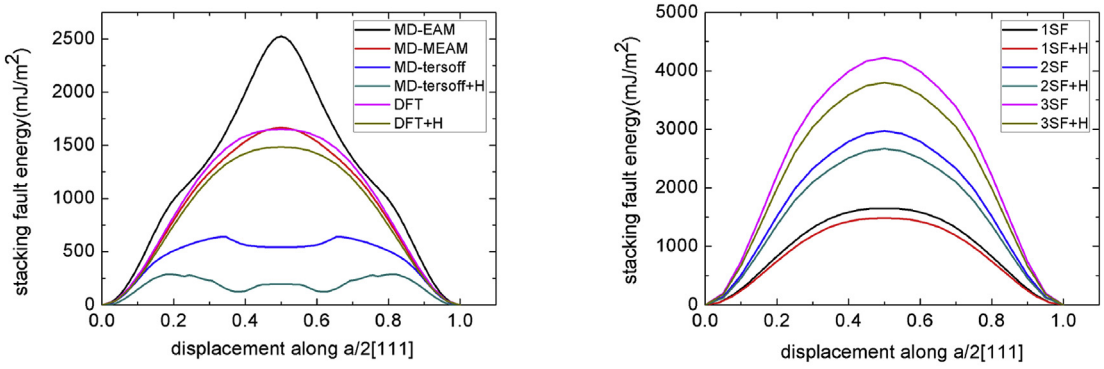

Fig. 5. The generalized stacking fault energy curves: (a) 1SF predicted by different methods. (b) 1SF, 2SF, and 3SF predicted by the QM method, both with and without H atoms.

The simulation reveals that $\frac{3G \cdot a^2}{32\pi(1-\nu)} = 5241.29 \times 10^{-10}$ mJ/m. From the above results, we obtain $\gamma \geq 1483.34$ mJ/m^2 with H added, then $d \leq 3.533$ Å, which indicates that the distance between the partial dislocations should be smaller than 3.533 Å. Clearly, no partial dislocations exist in H-doped bcc W systems. The WCH-tersoff potential predicted that $\gamma \approx 289.12$ mJ/m^2 with H, which suggested $d \approx 18.13$ Å. This value fits quite well with our simulation result, which could be attributed to the length scale provided in Fig. 3(c). Thus, we observed the stacking fault in the edge dislocation predicted by the WCH-tersoff potential and proved that it is not suitable for describing the relationship between the dislocation and H. Our stacking fault energy simulation revealed that no splitting behavior exists in bcc edge dislocation systems.

5. Conclusions

The multi-scale atomic simulations presented in this study combining QM and MD methods represent an efficient approach to address the problem of describing a large interval of relevant length in the study of the core structures of screw and edge dislocations in tungsten. The results indicate that the screw dislocation core in tungsten is a typical symmetric and non-polarized core and that the edge dislocation is complete. Indeed, both the screw and edge dislocation cores display limited changes after adding a column of H atoms to the dislocation core. The MD approach has its limitation, as the improper choice of potentials may result in failing to predict reasonable dislocation structures. Additionally, calculations of the generalized stacking fault energy suggest that the H atoms decrease the generalized stacking fault energy of tungsten but have almost no impact on the shape of the curve. This confirms the aforementioned results. The negligible disturbance of the tungsten lattice is attributed to the small size and limited concentration of interstitial H atoms. Further research may include the H cluster effects and the mobility of the dislocation influenced by certain concentrations of H atoms.

Acknowledgement

This work was supported by National Magnetic Confinement Fusion Science Program of China under Grant 2013GB109004 and 2014GB117000, and by National Natural Science Foundation of China under Grant 51471092.

References

[1] G. Leyson, B. Grabowski, J. Neugebauer, Acta Mater. 89 (2015) 50.
[2] J. von Pezold, L. Lymperakis, J. Neugebeauer, Acta Mater. 59 (2011) 2969.
[3] S. Wang, N. Hashimoto, S. Ohnuki, Sci. Rep. 3 (2013).
[4] D. Terentyev, V. Dubinko, A. Bakaev, Y. Zayachuk, W. Van Renterghem, P. Grigorev, Nucl. Fusion 54 (042004) (2014).
[5] P. Grigorev, D. Terentyev, G. Bonny, E.E. Zhurkin, G. Van Oost, J.-M. Noterdaeme, J. Nucl. Mater. 465 (2015) 364.
[6] X. Yang, A. Hassanein, J. Nucl. Mater. 434 (2013a) 1.
[7] Y. Liu, G. Lu, Z. Chen, N. Kioussis, Model. Simul. Mater. Sci. Eng. 15 (2007) 275.
[8] Hirth, J.; Lothe, J., Ed.: John Willey & Sons (1982).
[9] M. Fuchs, M. Scheffler, Comput. Phys. Commun. 119 (1999) 67.
[10] G. Kresse, J. Hafner, Phys. Rev. B 48 (1993) 13115.
[11] G. Kresse, J. Furthmüller, Comput. Mater. Sci. 6 (1996) 15.
[12] G. Kresse, D. Joubert, Phys. Rev. B 59 (1999) 1758.
[13] P.E. Blöchl, Phys. Rev. B 50 (1994) 17953.
[14] H.J. Monkhorst, J.D. Pack, Phys. Rev. B 13 (1976) 5188.
[15] X. Zhou, H. Wadley, R.A. Johnson, D. Larson, N. Tabat, A. Cerezo, A. Petford-Long, G. Smith, P. Clifton, R. Martens, et al., Acta mater. 49 (2001) 4005.
[16] D. Cereceda, A. Stukowski, M. Gilbert, S. Queyreau, L. Ventelon, M.-C. Marinica, J. Perlado, J. Marian, J. Phys. Condens. Matter 25 (2013) 085702.
[17] X. Yang, A. Hassanein, Nucl. Instrum. Methods Phys. Res. Sect. B Beam Interact. Mater. Atoms 308 (2013b) 80.
[18] N. Choly, G. Lu, E. Weinan, E. Kaxiras, Phys. Rev. B 71 (2005) 094101.
[19] S. Plimpton, J. Comput. Phys. 117 (1995) 1.
[20] L. Ventelon, B. Lüthi, E. Clouet, L. Proville, B. Legrand, D. Rodney, F. Willaime, Phys. Rev. B 91 (2015) 220102.
[21] C.D. Taylor, P. Marcus, Molecular Modeling of Corrosion Processes: Scientific Development and Engineering Applications, John Wiley & Sons, 2015.
[22] M. a.-S. Duesbery, V. Vitek, Acta Mater. 46 (1998) 1481.
[23] G.D. Samolyuk, Y. Osetsky, R. Stoller, J. Phys. Condens. Matter 25 (2012) 025403.
[24] C.S. Hartley, Y. Mishin, Mater. Sci. Eng. A 400 (2005) 18.
[25] F. Dai, W. Zhang, Acta Metall. Sin. (Engl. Lett.) 27 (2014) 1078.
[26] A. Machová, G.E. Beltz, M. Chang, Model. Simul. Mater. Sci. Eng. 7 (1999) 949.
[27] V. Vitek, Philos. Mag. 84 (2004) 415.
[28] D. Hull, D.J. Bacon, Introduction to Dislocations, vol. 37, Elsevier, 2011.
[29] D. Steinberg, S. Cochran, M. Guinan, J. Appl. Phys. 51 (1980) 1498.
[30] P.-O. Renault, K. Badawi, L. Bimbault, P. Goudeau, E. Elkaım, J. Lauriat, Appl. Phys. Lett. 73 (1998) 1952.